RESEARCH ARTICLE

Optimal concentration of necrostatin-1 for protecting against hippocampal neuronal damage in mice with status epilepticus

Dong-Qi Lin[1, 2], Xin-Ying Cai[3], Chun-Hua Wang[2], Bin Yang[2], Ri-Sheng Liang[2, *]

1 Department of Cardiothoracic Surgery, the Second Affiliated Hospital of Shantou University Medical College, Shantou, Guangdong Province, China

2 Department of Neurosurgery, Union Hospital, Fujian Medical University, Fuzhou, Fujian Province, China

3 Clinical Research Center, Shantou Central Hospital, Affiliated Shantou Hospital of Sun Yat-sen University, Shantou, Guangdong Province, China

Funding: *This study was supported by the Key Discipline Construction Project of the Union Hospital of Fujian Province, China, No. Δ211002#.*

Graphical Abstract

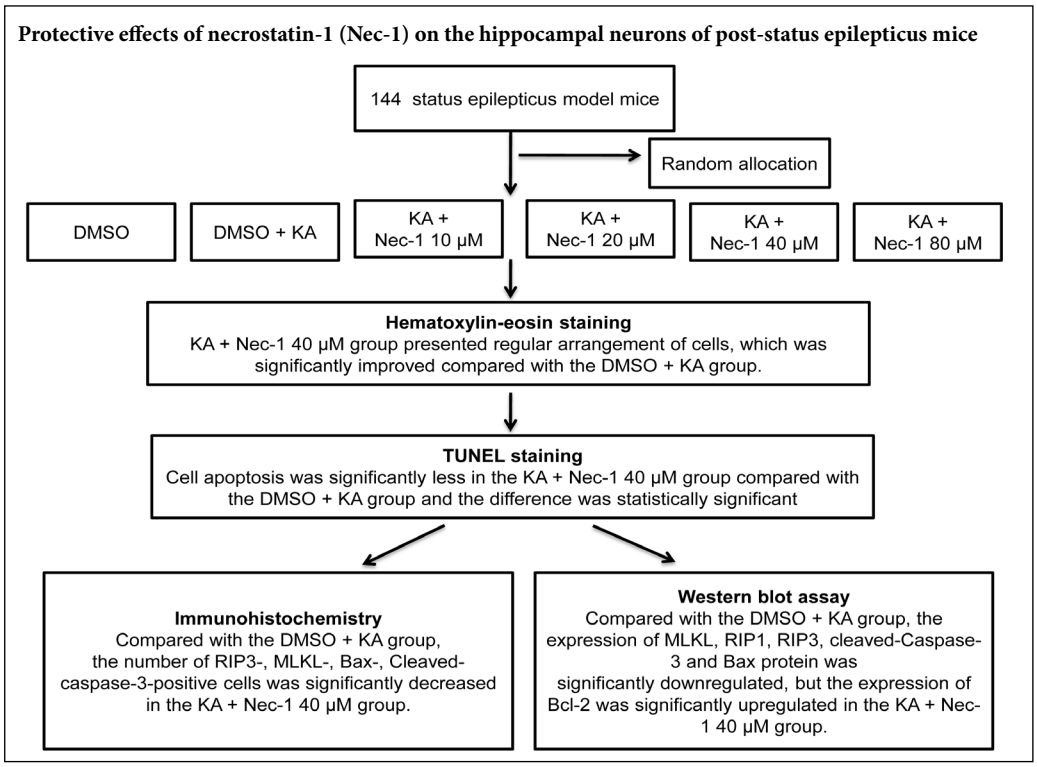

Correspondence to:
Ri-Sheng Liang, MD, doctorlr@126.com.

orcid:
0000-0002-1937-7188 (Ri-Sheng Liang)
0000-0002-9133-4502 (Dong-Qi Lin)

doi: *10.4103/1673-5374.268903*

Received: *March 2, 2019*
Peer review started: *March 10, 2019*
Accepted: *August 13, 2019*
Published online: *November 8, 2019*

Abstract

Hippocampal neurons undergo various forms of cell death after status epilepticus. Necrostatin-1 specifically inhibits necroptosis mediated by receptor interacting protein kinase 1 (RIP1) and RIP3 receptors. However, there are no reports of necroptosis in mouse models of status epilepticus. Therefore, in this study, we investigated the effects of necrostatin-1 on hippocampal neurons in mice with status epilepticus, and, furthermore, we tested different amounts of the compound to identify the optimal concentration for inhibiting necroptosis and apoptosis. A mouse model of status epilepticus was produced by intraperitoneal injection of kainic acid, 12 mg/kg. Different concentrations of necrostatin-1 (10, 20, 40, and 80 μM) were administered into the lateral ventricle 15 minutes before kainic acid injection. Hippocampal damage was assessed by hematoxylin-eosin staining 24 hours after the model was successfully produced. Terminal deoxynucleotidyl transferase-mediated dUTP nick end labeling staining, western blot assay and immunohistochemistry were used to evaluate the expression of apoptosis-related and necroptosis-related proteins. Necrostatin-1 alleviated damage to hippocampal tissue in the mouse model of epilepsy. The 40 μM concentration of necrostatin-1 significantly decreased the number of apoptotic cells in the hippocampal CA1 region. Furthermore, necrostatin-1 significantly downregulated necroptosis-related proteins (MLKL, RIP1, and RIP3) and apoptosis-related proteins (cleaved-Caspase-3, Bax), and it upregulated the expression of anti-apoptotic protein Bcl-2. Taken together, our findings show that necrostatin-1 effectively inhibits necroptosis and apoptosis in mice with status epilepticus, with the 40 μM concentration of the compound having an optimal effect. The experiments were approved by the Animal Ethics Committee of Fujian Medical University, China (approval No. 2016-032) on November 9, 2016.

Key Words: *apoptosis; Bax; Bcl-2; cleaved-Caspase-3; epilepsy; hippocampal neuron; MLKL; necroptosis; necrostatin-1; nerve regeneration; neural regeneration; RIP1; RIP3*

Chinese Library Classification No. *R453; R363; R364*

Introduction

Epilepsy is a common highly debilitating neurological disease characterized by the abnormal discharge of brain neurons (Filippov and Vorobyov, 2019). Necrosis and apoptosis are the major forms of neuronal death post-epilepsy (Zhang et al., 2014).

Recent studies show that necroptosis is a form of regulated cell death (Christofferson and Yuan, 2010; Pan et al., 2019; Shi et al., 2019; Yuan et al., 2019). Necroptosis is regulated by complex IIb, which is composed of RIP1 and RIP3, proteins that interact through the RIP homotypic interaction motif, while MLKL is a key downstream regulator of RIP3 kinase (Baker et al., 2018; Johnston and Wang, 2018; Ni et al., 2019; Wang et al., 2019). Necroptosis has been observed in a variety of diseases, including central nervous system diseases (Ofengeim et al., 2015; Yang et al., 2018), ischemia/reperfusion injury (Oerlemans et al., 2012; Hribljan et al., 2019; Li et al., 2019; Liu et al., 2019), and acute inflammation (Newton et al., 2014). However, there is no report of necroptosis in a mouse model of epilepsy.

Brain damage caused by seizures is mainly produced by neuronal apoptosis (Polster and Fiskum, 2004; Wang et al., 2016; Panda et al., 2018; Xu et al., 2019; Zhou et al., 2019), and Caspase-3 is the ultimate effector of the apoptotic signaling pathway (Yang et al., 2018). In addition, the anti-apoptotic protein Bcl-2 can reverse sudden brain damage (Graham et al., 2000). Bcl-2 attenuates status epilepticus-induced neuronal damage by inhibiting the Caspase-3-dependent proteolytic enzyme cascade. Bax, an important pro-apoptotic protein (Tuunanen et al., 1999), induces translocation of cytochrome C across the mitochondrial membrane, thereby activating Caspase-9, which in turn activates Caspase-3, resulting in apoptosis.

Necrostatin-1 (Nec-1) is a small molecule compound that blocks programmed necrosis by specifically inhibiting RIP1 (Degterev et al., 2005, 2008; Song et al., 2019). Numerous studies have shown that Nec-1 exerts neuroprotective effects in various models of neural injury (You et al., 2008; Xu et al., 2010; Yang et al., 2019). However, its neuroprotective effect in epilepsy models remains unclear. In this study, we investigate the effect of Nec-1 on neuronal necroptosis-related signaling pathways in mice with kainic acid (KA)-induced epilepsy. Furthermore, we screen for the optimal concentration of Nec-1 that inhibits apoptosis and necroptosis. Our findings should advance our understanding of the pathogenesis of epilepsy and help identify new therapeutic targets for the disorder.

Materials and Methods

Animals

A total of 144 specific-pathogen-free adult male Institute of Cancer Research (ICR) mice, weighing 22–28 g, were provided by the Shanghai Laboratory Animal Center, Chinese Academy of Sciences, Shanghai, China (animal license number: SCXK (Hu)-2012-0002). The experiments were approved by the Institutional Animal Care and Use Committees of Fujian Medical University, China (approval No. 2016-032) on November 9, 2016. The experimental procedure followed the United States National Institutes of Health Guide for the Care and Use of Laboratory Animals (NIH Publication No. 85-23, revised 1996). The animals were housed in a room maintained at 22–26°C, humidity of 50–60%, with good ventilation, under a 12/12-hour light/dark cycle. The mice were allowed free access to food and water. All animals were acclimated to the experimental environment for one week before the experiments.

The 144 mice were divided into six groups (n = 24 each). In the dimethyl sulfoxide (DMSO) group, DMSO was injected into the lateral ventricle, and 15 minutes later, saline was injected into the abdominal cavity. Then, 24 hours later, the mice were killed. In the DMSO + KA group, DMSO was injected into the lateral ventricle, and 15 minutes later, KA was injected into the abdominal cavity. Then, 24 hours later, the mice were killed. In the KA + Nec-1 10, 20, 40 and 80 μM groups, 10, 20, 40 or 80 μM Nec-1 + DMSO was injected into the lateral ventricle, and 15 minutes later, KA was injected into the abdominal cavity. Then, 24 hours later, the mice were killed.

Production of the mouse model of status epilepticus

All surgical procedures were performed under aseptic conditions. The mouse model of status epilepticus was produced by KA injection (12 mg/kg; Cayman Chemical, Ann Arbor, MI, USA) into the abdominal cavity. This effective concentration was established in previous experiments. Before abdominal injection, isoflurane inhalation anesthesia was given, and the mice were injected with DMSO (1 μL; Sinopharm Chemical Reagent Co., Ltd., Shanghai, China). Each group was given the same KA injection, with no treatment for the DMSO group. Under normal conditions, mice would exhibit Racine stage 5 seizures (characterized by rearing and falling) 1 hour after KA injection (Liao et al., 2016).

Drug administration

Nec-1 (purity: > 98%; CAS No. 4311-88-0, Sigma-Aldrich, St. Louis, MO, USA) was dissolved in DMSO (Sinopharm Chemical Reagent Co., Ltd.) to 10, 20, 40 or 80 μM (Wu et al., 2015). Mice were pre-injected with the Nec-1/DMSO solution into the lateral ventricles under a stereotaxic microscope (Olympus, Tokyo, Japan). The mice were placed on the stereotaxic apparatus (Olympus), anesthetized with isoflurane (Sinopharm Chemical Reagent Co., Ltd.), and a cut was made along the midline of the scalp to expose the bregma. A hole was drilled in the skull, and the trocar was positioned (relative to the bregma, anteroposterior ± 1.9 mm, midline ± 2.1 mm) on the stereotaxic apparatus. The trocar was descended 2.4 mm from the brain surface into the lateral ventricle, and the Nec-1/DMSO solution, 1 μL, was injected. In the DMSO + KA and DMSO groups, the same volume of DMSO was injected into the lateral ventricle. During the entire surgical procedure, the anal temperature was maintained at 37°C with heating plates and lamps.

Before removal of the hippocampus, the mice were treated with chloral hydrate (10%, 600 mg/kg, 3.5 mL/kg, intraperitoneally). Chloral hydrate was chosen because it has not been shown to upregulate autophagy compared with other anesthetics (Kashiwagi et al., 2015). The chloral hydrate dose was chosen according to a previous study (Li et al., 2016) that reported the duration of maintenance, recovery time, heart rate, and mortality. The anesthesia protocol followed the American Veterinary Association and the British Animal Act guidelines to effectively reduce pain and suffering (Kelch, 2001; Chen et al., 2014).

Hematoxylin-eosin staining

A total of 36 mice were used for hematoxylin-eosin staining (n = 6 for each group). After 24 hours of epileptic seizures, mice were anesthetized with chloral hydrate (10%, 600 mg/kg, 3.5 mL/kg, intraperitoneally), and then perfused with physiological saline. Brain tissue was fixed with 4% paraformaldehyde. After the mice were decapitated, the brain tissue was embedded in paraffin and cut into 5–6-mm sections containing the hippocampus, and then further cut into 30-μm coronal sections with a microtome. The sections were then put through a graded alcohol series, dewaxed in dimethyl benzene, and stained with hematoxylin and eosin. The sections were then transferred to glass slides and mounted with neutral balsam (ZLI-9516; Zhongshan Golden Bridge Biotechnology Co., Ltd., Beijing, China).

TUNEL staining

Terminal deoxynucleotidyl transferase-mediated dUTP nick end-labeling (TUNEL) assay (Promega Corporation, Fitchburg, WI, USA) was used to detect apoptosis in the hippocampal CA1 area, in accordance with the manufacturer's instructions. After 24 hours of epileptic seizures, 36 mice (n = 6 for each group) were killed. After paraffin embedding, tissue sections were incubated with proteinase K (Zhongshan Golden Bridge Biotechnology Co., Ltd.) for 10–30 minutes at room temperature. The sections were placed in equilibration buffer, incubated with rTdT solution (Promega Corporation) at 37°C for 60 minutes, and washed with 2× SSC at room temperature for 15 minutes. Hydrogen peroxide, 0.3%, was added, and then incubated with horseradish peroxidase-labeled streptavidin (Zhongshan Golden Bridge Biotechnology Co., Ltd.) in phosphate-buffered saline at room temperature for 30 minutes. The sections were then incubated with 3,3′-diaminobenzidine (Zhongshan Golden Bridge Biotechnology Co., Ltd.) and counterstained with hematoxylin (Zhongshan Golden Bridge Biotechnology Co., Ltd.). Sections were rinsed with deionized water, dried, and sealed with neutral balsam. The brown (apoptotic) cells in the hippocampal CA1 area were observed under the light microscope (Olympus). The numbers of apoptotic cells in the whole CA1 area in three consecutive sections were counted, and the average percentage of positive cells was calculated at 400× magnification.

Immunohistochemistry

After 24 hours of epileptic seizures, 36 mice (n = 6 for each group) were used for immunohistochemistry. The animal was decapitated, and the brain was harvested and embedded in paraffin. The tissue was dewaxed through a graded alcohol series, treated with 0.3% hydrogen peroxide solution for 10 minutes, and then incubated with diluted primary antibodies overnight at 4°C. The primary antibodies were as follows: anti-RIP3 (necroptosis pathway-related protein; 1:200; monoclonal rabbit antibody; Sigma-Aldrich), anti-MLKL (necroptosis-related protein; 1:200; monoclonal rabbit antibody; Abcam, Cambridge, UK), anti-cleaved-caspase3 (pro-apoptotic protein; 1:150; monoclonal rabbit antibody; Cell Signaling Technology, Abcam Trading, Shanghai, China), and anti-Bax (pro-apoptotic protein; 1:150; monoclonal rabbit antibody; Cell Signaling Technology). Sections were incubated with the primary antibodies at 4°C overnight, and then with horseradish peroxidase-labeled goat anti-rabbit IgG (1:200; Zhongshan Golden Bridge Biotechnology Company, Beijing, China) at room temperature for 60 minutes. Thereafter, 3,3′-diaminobenzidine solution was added and quickly rinsed after sufficient color development. The sections were then counterstained and sealed. Image-Pro Plus software (Media Cybernetics, Bethesda, MD, USA) was used to assess staining intensity. The hippocampi of the DMSO group were used as a positive internal control. Immunohistochemical results were interpreted with the assistance of a pathologist. The percentages of cleaved-Caspase-3 and Bax-positive cells in the hippocampus were recorded for each section. Hippocampal cells were considered positively stained even when the intensity of staining varied or was membranous or cytoplasmic.

Western blot assay

A total of 36 mice (n = 6 for each group) were used for western blot assay. After 24 hours of epileptic seizures, the brain was harvested, and protein from the bilateral hippocampi was extracted and quantified using a bicinchoninic acid protein assay kit (Beyotime Biotechnology, Shanghai, China). Electrophoresis was conducted, and the proteins were blotted onto a polyvinylidene fluoride membrane. After blocking, the membrane was rinsed with Tris-buffered saline/Tween (TBST), and then incubated with primary antibody (**Table 1**). The membrane was washed with TBST and incubated with secondary antibodies (**Table 1**). Then, after washing with TBST, the membrane was reacted with enhanced chemiluminescence reagent. Band intensities were visualized using Image Station 4000 MM imager. β-Actin was used as the internal control. Data were analyzed with a western blot analysis system (Carestream Company, Toronto, Canada).

Statistical analysis

Statistical analysis was conducted with SPSS 17.0 software (SPSS, Chicago, IL, USA). Data were normally distributed and are expressed as the mean ± SD. All data are analyzed by one-way analysis of variance followed by Tukey's *post hoc* test. $P < 0.05$ was considered statistically significant.

Table 1 Antibodies of western blot assay

	Primary antibodies	Secondary antibodies
Necroptosis-related pathway protein antibodies	Anti-RIP1 (1:1000; monoclonal rabbit antibody; Santa Cruz Biotechnology, Dallas, TX, USA)	Horseradish peroxidase-labeled goat anti-rabbit IgG (1:2000; Zhongshan Golden Bridge Biotechnology Company, Beijing, China)
	Anti-RIP3 (1:2000; monoclonal rabbit antibody; Sigma-Aldrich, St. Louis, MO, USA)	Horseradish peroxidase-labeled goat anti-rabbit IgG (1:2000; Zhongshan Golden Bridge Biotechnology Company)
	Anti-MLKL (1:2000; monoclonal rabbit antibody; Abcam, Cambridgeshire, UK)	Horseradish peroxidase-labeled goat anti-rabbit IgG (1:2000; Zhongshan Golden Bridge Biotechnology Company)
Pro-apoptosis antibodies	Anti Bcl 2 (1:2000; monoclonal rabbit antibody; Beyotime Biotechnology, Shanghai, China)	Horseradish peroxidase-labeled goat anti-rabbit IgG (1:2000; Zhongshan Golden Bridge Biotechnology Company)
	Anti-cleaved-Caspase-3 (1:800; monoclonal rabbit antibody; Cell Signaling Technology, Inc., Danvers, MA, USA)	Horseradish peroxidase-labeled goat anti-rabbit IgG (1:2000; Zhongshan Golden Bridge Biotechnology Company)
Anti-apoptosis antibodies	Anti-Bax (1:800; monoclonal rabbit antibody; Cell Signaling Technology, Inc.).	Horseradish peroxidase-labeled goat anti-rabbit IgG (1:2000; Zhongshan Golden Bridge Biotechnology Company)
Internal reference antibody	β-Actin monoclonal antibody (1:1000; monoclonal mouse antibody; Cell Signaling Technology, Inc.)	Horseradish peroxidase-labeled goat anti-mouse IgG (1:2000; Zhongshan Golden Bridge Biotechnology Company)

Results

Status epilepticus

After KA injection into the abdominal cavity, mice gradually developed epileptic seizures that lasted for 1–3 hours. During seizures, mice initially exhibited whisker-quivering, mastication, blinks and wet dog shakes, and then head nodding, whirling, one-sided forelimb clonus and other stage II–III manifestations. As the seizures progressed, mice gradually displayed rearing, double forelimb tremor, body dorsiflexion, falling, and limb convulsion, which worsened into grand mal, and then status epilepticus. No seizures were observed in the DMSO group.

Damage to hippocampal cells in mice with status epilepticus detected by hematoxylin-eosin staining

The morphological changes in CA1 cells were observed with hematoxylin-eosin staining. As shown in **Figure 1**, in the DMSO group, normal morphology and structure of the hippocampus were found. The cells were neatly arranged and evenly colored, the sizes of the nuclei and nucleoli were normal, and the cytoplasm and nuclei were brightly stained, light red and light blue. In the DMSO + KA group, cellular morphology and hippocampal structure were abnormal. Pyramidal cells were lost, the cytoplasm was transparent, the nucleus and cytoplasm were stained dark blue and purple-blue, with uneven coloring, and the cells were of different sizes and morphologies. Some neurons were swollen and vacuolated, while others had shrunk in size. The nuclei showed signs of pyknosis and hyperchromatism. The nucleoli were small or missing. The cells appeared necrotic. After Nec-1 treatment, the cells appeared more normal, and the hyperchromatism and nuclear shrinkage were reduced. Notably, among the various groups, the Nec-1 40 μM group showed a regular arrangement of cells, which was significantly improved compared with the DMSO + KA group.

Neuronal apoptosis in the hippocampus in mice with status epilepticus detected by TUNEL staining

There was a small number of brown apoptotic granule cells in the DMSO group. After status epilepticus, the number of brown apoptotic cells in the hippocampal CA1 area was significantly increased ($P < 0.05$). The number of apoptotic cells was significantly less in the KA + Nec-1 40 μM group than in the DMSO + KA group ($P < 0.001$; **Figure 2**).

Assessment and quantification of target proteins by immunohistochemistry

The DMSO group showed a small number of scattered Bax, cleaved-Caspase-3, MLKL and RIP3-positive cells in the hippocampal CA1 area (**Figures 3** and **4**). Compared with the DMSO group, the DMSO + KA group had a large amount of RIP3, MLKL, Bax and cleaved-Caspase-3-positive cells, and these cells were arranged irregularly and densely ($P < 0.05$). Compared with the DMSO + KA group, the KA + Nec-1 40 μM group showed significantly less RIP3, MLKL, Bax and cleaved-Caspase-3-positive cells. Furthermore, the cells had a lightly stained membrane and cytoplasm, which were pale brown ($P < 0.01$).

Assessment and quantification of target proteins by western blot assay

The DMSO group showed weak expression of MLKL, RIP1, RIP3, cleaved-Caspase-3 and Bax proteins and high levels of expression of Bcl-2 protein (**Figure 5A–D**). Expression levels of MLKL, RIP1, RIP3, cleaved-Caspase-3 and Bax protein were significantly higher, while Bcl-2 protein levels were significantly lower, in the DMSO + KA group compared with the DMSO group ($P < 0.05$). Compared with the DMSO + KA group, the expression of MLKL, RIP1, RIP3, cleaved-Caspase-3 and Bax protein in the hippocampus was significantly downregulated ($P < 0.01$), while Bcl-2 protein was significantly upregulated, in the KA + Nec-1 40 μM group ($P < 0.05$; **Figure 5E–H**).

Discussion

The use of male mice in this study was in accordance with previous studies (Chavez-Valdez et al., 2014; Liao et al., 2016; Sowndhararajan et al., 2018). Nec-1 only has a protective effect against ischemic/hypoxic brain damage in male newborns (Chavez-Valdez et al., 2014, 2019). In the report of Chavez-Valdez et al., Nec-1 decreased cell death receptor

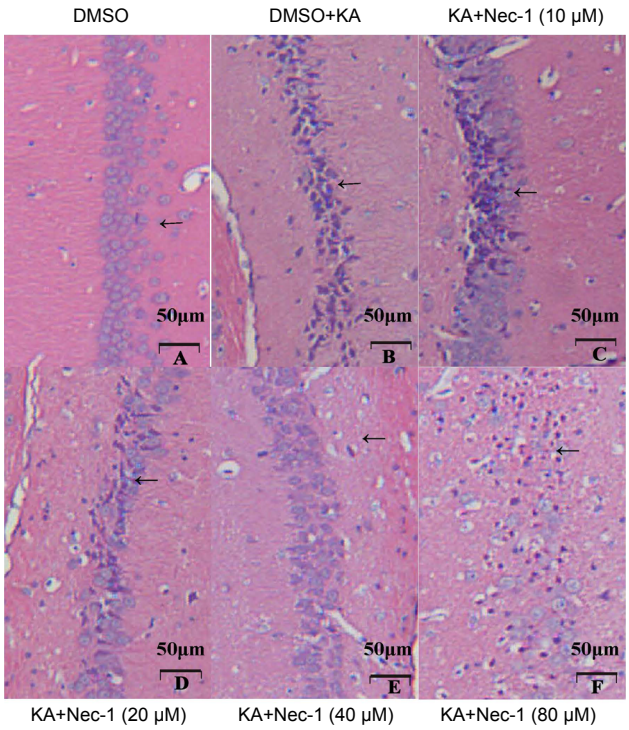

Figure 1 Effect of necrostatin-1 on pathological changes in hippocampal tissue (CA1) in status epilepticus mice.
Sections were examined with optical microscopy to assess morphological changes in the CA1 by hematoxylin-eosin staining. The nucleus underwent pyknosis and hyperchromatism. The nucleolus became small or even disappeared, and the morphology of cells showed signs of necrosis (arrows). Scale bars: 50 μm. DMSO: Dimethyl sulfoxide; KA: kainic acid; Nec-1: necrostatin-1.

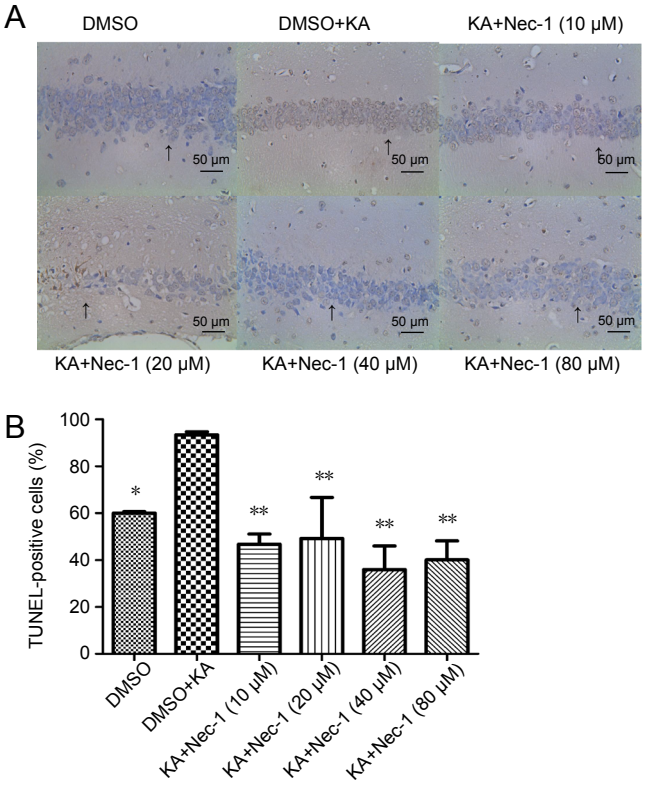

Figure 2 Effects of necrostatin-1 on cell apoptosis in the hippocampal CA1 area in status epilepticus mice.
(A) Cellular apoptosis (arrows) in the hippocampus was assessed by terminal deoxynucleotidyl transferase-mediated dUTP nick end labeling (TUNEL) staining. Scale bars: 50 μm. (B) The percentage of TUNEL-positive cells in each group. Data are expressed as the mean ± SD (n = 6; one-way analysis of variance followed by Tukey's *post hoc* test). *P < 0.05, **P < 0.01, *vs.* DMSO + KA group. DMSO: Dimethyl sulfoxide; KA: kainic acid; Nec-1: necrostatin-1.

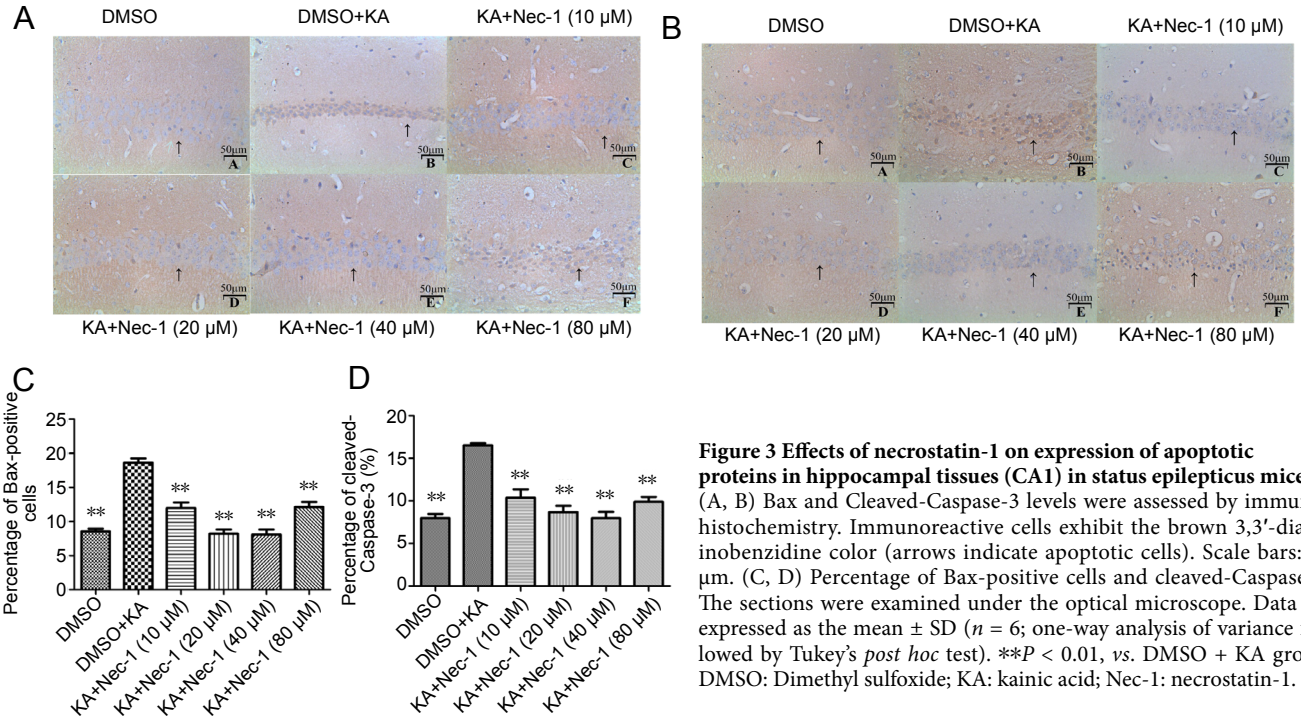

Figure 3 Effects of necrostatin-1 on expression of apoptotic proteins in hippocampal tissues (CA1) in status epilepticus mice.
(A, B) Bax and Cleaved-Caspase-3 levels were assessed by immunohistochemistry. Immunoreactive cells exhibit the brown 3,3′-diaminobenzidine color (arrows indicate apoptotic cells). Scale bars: 50 μm. (C, D) Percentage of Bax-positive cells and cleaved-Caspase-3. The sections were examined under the optical microscope. Data are expressed as the mean ± SD (n = 6; one-way analysis of variance followed by Tukey's *post hoc* test). **P < 0.01, *vs.* DMSO + KA group. DMSO: Dimethyl sulfoxide; KA: kainic acid; Nec-1: necrostatin-1.

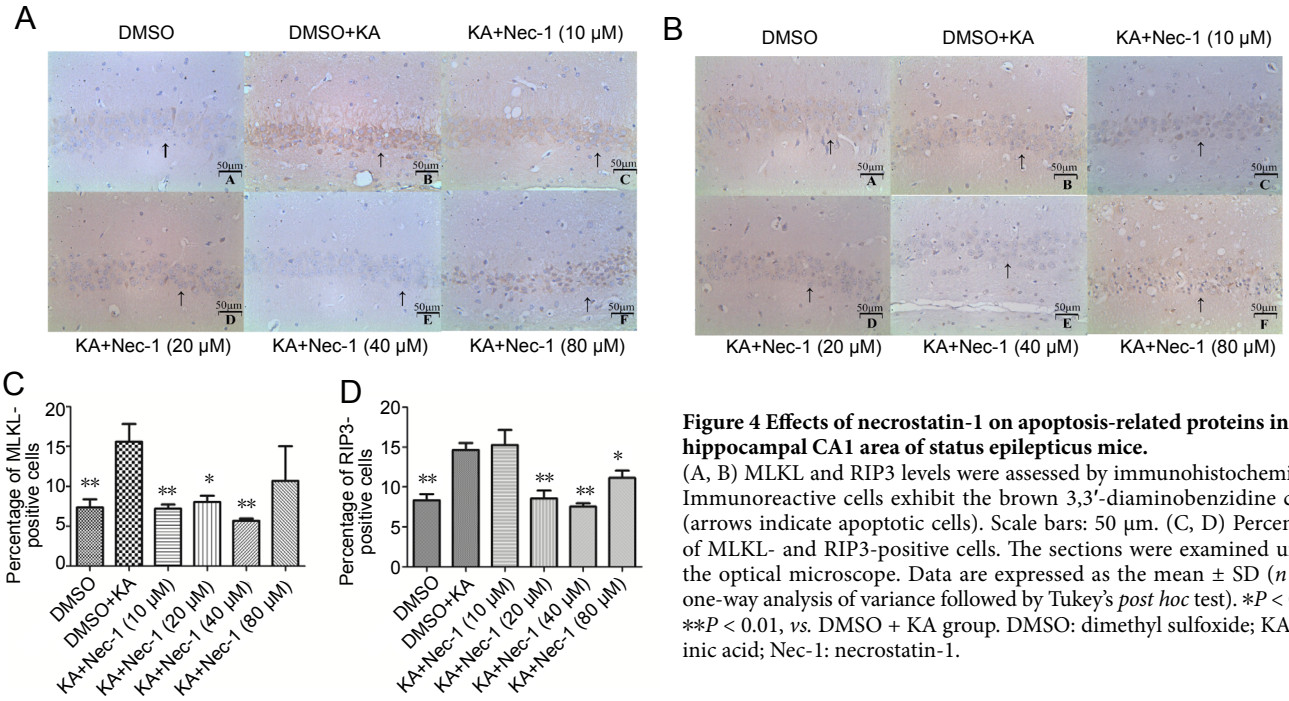

Figure 4 Effects of necrostatin-1 on apoptosis-related proteins in the hippocampal CA1 area of status epilepticus mice.
(A, B) MLKL and RIP3 levels were assessed by immunohistochemistry. Immunoreactive cells exhibit the brown 3,3′-diaminobenzidine color (arrows indicate apoptotic cells). Scale bars: 50 μm. (C, D) Percentage of MLKL- and RIP3-positive cells. The sections were examined under the optical microscope. Data are expressed as the mean ± SD (n = 6; one-way analysis of variance followed by Tukey's *post hoc* test). ∗P < 0.05, ∗∗P < 0.01, *vs.* DMSO + KA group. DMSO: dimethyl sulfoxide; KA: kainic acid; Nec-1: necrostatin-1.

proteins (Tc.TrkB and $p75^{NTR}$) in female mice, but the underlying mechanism was unclear. Therefore, we only used male mice in the current study.

KA injection into the abdominal cavity was used to induce status epilepticus and cause neuronal damage, and the injured hippocampal neurons underwent a considerable amount of apoptosis and necroptosis (Kondratyev and Gale, 2000). We found that the expression levels of RIP1, RIP3, MLKL, cleaved-Caspase-3 and Bax in the hippocampus of post-epileptic mice were significantly increased, while the expression of Bcl-2 protein was decreased, suggesting that hippocampal neurons undergo death through apoptosis and necroptosis after status epilepticus.

RIPK3 and MLKL are important mediators of necroptosis (Yang et al., 2015; Sai et al., 2019; Zhang and Balachandran, 2019; Zhang et al., 2019a, b). In mouse models of KA-induced epilepsy, there are few reports on the mechanism of Nec-1-mediated neuroprotection of hippocampal cells (Arrázola et al., 2019). Nec-1 inhibits necroptosis by inhibiting RIPK1 and blocking the interaction of RIPK1 with RIPK3. Western blot assay and immunohistochemical staining showed that the expression of RIP1, RIP3 and MLKL, factors related to necroptosis, in the hippocampus was significantly increased after KA-induced epilepsy in mice. RIP1, RIP3 and MLKL were significantly downregulated after treatment with Nec-1 (40 μM). These results suggest that Nec-1 may protect hippocampal neurons in mice by inhibiting necroptosis. Nec-1 not only reduced the number of apoptotic cells, but also significantly downregulated cleaved-Caspase-3 and Bax, and upregulated Bcl-2. To the best of our knowledge, this is the first demonstration of a role for Nec-1 in inhibiting apoptosis and necroptosis in a mouse model of epilepsy.

However, further study is needed to more fully elucidate the mechanisms underlying the neuroprotection provided by Nec-1.

In future studies, we anticipate including animal behavioral and brain imaging studies to further clarify the neuroprotective effects of Nec-1. The study of animal behavior is key to understanding the biological effects of drugs and their molecular targets (Puzzo et al., 2014). Imaging is widely used to study animal models. Photoacoustic and thermoacoustic imaging is currently a research hotspot in the field of medical imaging. These techniques have advanced the study of brain hemodynamics, brain activity, and even brain function (Zeng et al., 2004, 2007; He et al., 2006; Zhang et al., 2006).

In summary, our study clarifies the neuroprotective mechanism of action of Nec-1 on brain damage in mice with KA-induced epilepsy. Nec-1 effectively inhibited programmed necrosis and apoptosis at a concentration of 40 μM. Therefore, the 40 μM concentration is the optimal therapeutic concentration for Nec-1 to protect neurons against necroptosis and apoptosis.

Author contributions: *Data collection, paper writing: DQL, XYC; experiment support: CHW; experiment operation: BY; study design and guidance: RSL. All authors approved the final version of the study.*
Conflicts of interest: *The authors declare that there are no conflicts of interest associated with this manuscript.*
Financial support: *The study was supported by the Key Discipline Construction Project of the Union Hospital of Fujian Province, China, No. Δ211002#. The funding sources had no role in study conception and design, data analysis or interpretation, paper writing or deciding to submit this paper for publication.*
Institutional review board statement: *The experiment was performed in accordance with approval of the Institutional Animal Care and Use Committees of Fujian Medical University, China (approval No. 2016-032) on November 9, 2016.*
Copyright license agreement: *The Copyright License Agreement has been signed by all authors before publication.*
Data sharing statement: *Datasets analyzed during the current study are available from the corresponding author on reasonable request.*
Plagiarism check: *Checked twice by iThenticate.*
Peer review: *Externally peer reviewed.*
Open access statement: *This is an open access journal, and articles are*

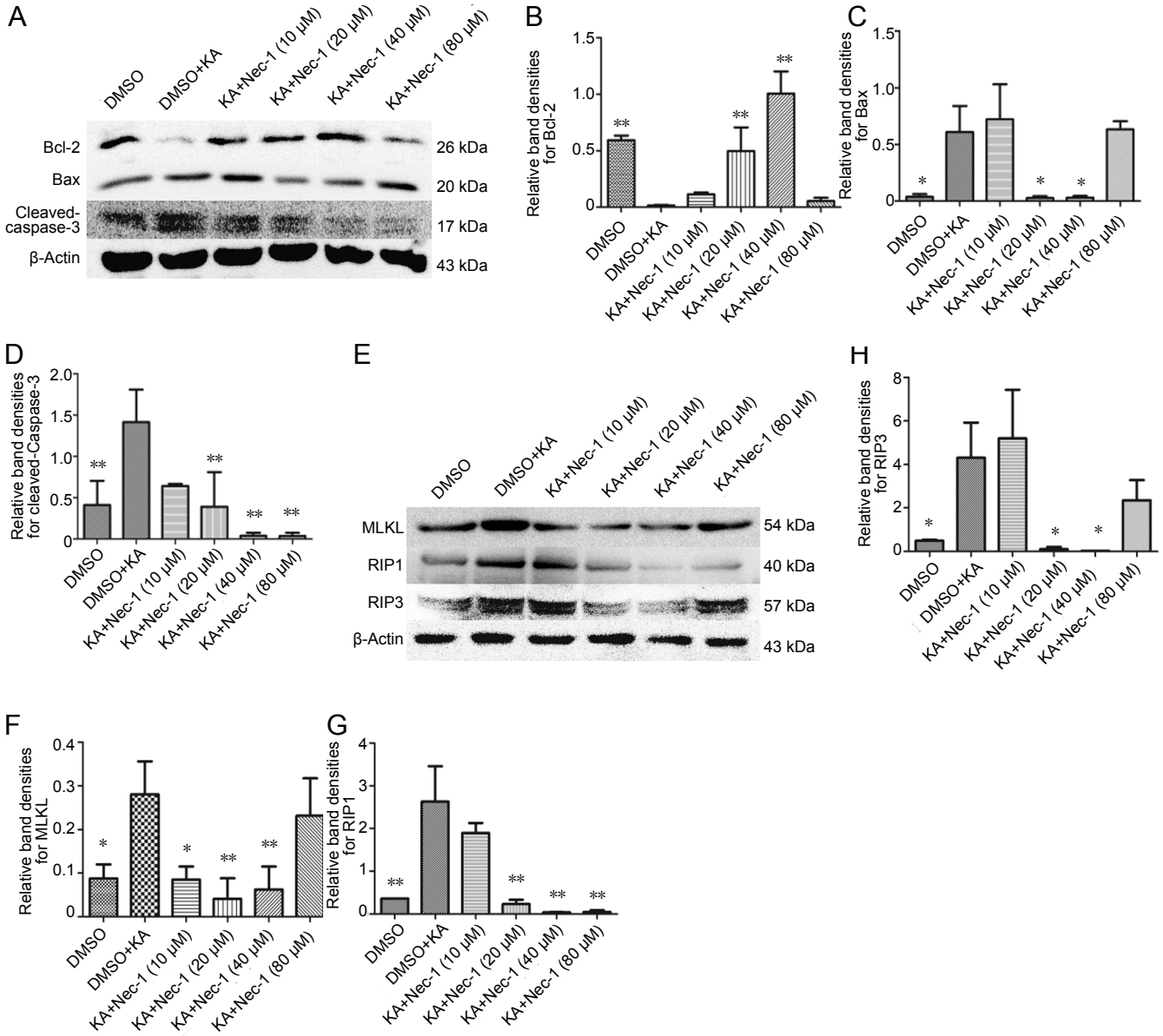

Figure 5 Effects of necrostatin-1 on apoptotic protein expression in hippocampal cells (CA1) in status epilepticus mice.
(A) Western blot assay for cleaved-Caspase-3, Bax and Bcl-2. (B–D) Relative band densities for Bcl-2, Bax, and cleaved-Caspase-3. (E) Western blot assay for MLKL, RIP1 and RIP3. (F–H) Relative band densities for MLKL, RIP1 and RIP3. The grayscales were normalized to β-actin. Data are expressed as the mean ± SD (n = 6; one-way analysis of variance followed by Tukey's *post hoc* test). ∗P < 0.05, ∗∗P < 0.01, *vs.* DMSO + KA group. DMSO: Dimethyl sulfoxide; KA: kainic acid; Nec-1: necrostatin-1; RIP1: receptor interacting protein kinase 1; RIP: receptor interacting protein kinase.

Open peer reviewer: *Muneeb Faiq, New York University School of Medicine, USA; David Benn Lovejoy, Macquarie University Faculty of Medicine and Health Sciences, Biomedical Sciences, Australia.*
Additional file: *Open peer review reports 1 and 2.*

References

Arrázola MS, Saquel C, Catalán RJ, Barrientos SA, Hernandez DE, Martínez NW, Catenaccio A, Court FA (2019) Axonal degeneration is mediated by necroptosis activation. J Neurosci 39:3832-3844.

Baker MODG, Shanmugam N, Pham CLL, Strange M, Steain M, Sunde M (2018) RHIM-based protein:protein interactions in microbial defence against programmed cell death by necroptosis. Semin Cell Dev Biol doi:10.1016/j.semcdb.2018.05.004.

Chavez-Valdez R, Martin LJ, Razdan S, Gauda EB, Northington FJ (2014) Sexual dimorphism in BDNF signaling after neonatal hypoxia-ischemia and treatment with necrostatin-1. Neuroscience 260:106-119.

Chavez-Valdez R, Mottahedin A, Stridh L, Yellowhair TR, Jantzie LL, Northington FJ, Mallard C (2019) Evidence for sexual dimorphism in the response to tlr3 activation in the developing neonatal mouse brain: a pilot study. Front Physiol 10:306.

Chen SN, Chang CS, Hung MH, Chen S, Wang W, Tai CJ, Lu CL (2014) The effect of mushroom beta-glucans from solid culture of ganodermalucidum on inhibition of the primary tumor metastasis. Evid Based Complement Alternat Med 2014:252171.

Christofferson DE, Yuan J (2010) Necroptosis as an alternative form of programmed cell death. Curr Opin Cell Biol 22:263-268.
Degterev A, Hitomi J, Germscheid M, Ch'en IL, Korkina O, Teng X, Abbott D, Cuny GD, Yuan C, Wagner G, Hedrick SM, Gerber SA, Lugovskoy A, Yuan J (2008) Identification of RIP1 kinase as a specific cellular target of necrostatins. Nat Chem Biol 4:313-321.
Degterev A, Huang Z, Boyce M, Li Y, Jagtap P, Mizushima N, Cuny GD, Mitchison TJ, Moskowitz MA, Yuan J (2005) Chemical inhibitor of nonapoptotic cell death with therapeutic potential for ischemic brain injury. Nat Chem Biol 1:112-119.
Filippov MA, Vorobyov VV (2019) Detrimental and synergistic role of epilepsy-Alzheimer's disease risk factors. Neural Regen Res 14:1376-1377.
Graham SH, Chen J, Clark RS (2000) Bcl-2 family gene products in cerebral ischemia and traumatic brain injury. J Neurotrauma 17:831-841.
He Y, Tang Z, Chen Z, Wan W, Li J (2006) A novel photoacoustic tomography based on a time-resolved technique and an acoustic lens imaging system. Phys Med Biol 51:2671-2680.
Hribljan V, Lisjak D, Petrović DJ, Mitrečić D (2019) Necroptosis is one of the modalities of cell death accompanying ischemic brain stroke: from pathogenesis to therapeutic possibilities. Croat Med J 60:121-126.
Johnston A, Wang Z (2018) Necroptosis: MLKL Polymerization. J Nat Sci 4:e513.
Kashiwagi A, Hosokawa S, Maeyama Y, Ueki R, Kaneki M, Martyn JA, Yasuhara S (2015) Anesthesia with disuse leads to autophagy up-regulation in the skeletal muscle. Anesthesiology 122:1075-1083.
Kelch TG (2001) Animal experimentation and the first amendment. West New Engl Law Rev 22:2.
Kondratyev A, Gale K (2000) Intracerebral injection of caspase-3 inhibitor prevents neuronal apoptosis after kainic acid-evoked status epilepticus. Brain Res Mol Brain Res 75:216-224.
Li J, Zhang J, Zhang Y, Wang Z, Song Y, Wei S, He M, You S, Jia J, Cheng J (2019) TRAF2 protects against cerebral ischemia-induced brain injury by suppressing necroptosis. Cell Death Dis 10:328.
Li L, Tian J, Long MK, Chen Y, Lu J, Zhou C, Wang T (2016) Protection against experimental stroke by Ganglioside GM1 Is associated with the inhibition of autophagy. PLoS One 11:e0144219.
Liao ZJ, Liang RS, Shi SS, Wang CH, Yang WZ (2016) Effect of baicalin on hippocampal damage in kainic acid-induced epileptic mice. Exp Ther Med 12:1405-1411.
Liu H, Zhang MZ, Liu YF, Dong XH, Hao Y, Wang YB (2019) Necroptosis was found in a rat ischemia/reperfusion injury flap model. Chin Med J 132:42-50.
Newton K, Dugger DL, Wickliffe KE, Kapoor N, de Almagro MC, Vucic D, Komuves L, Ferrando RE, French DM, Webster J, Roose-Girma M, Warming S, Dixit VM (2014) Activity of protein kinase RIPK3 determines whether cells die by necroptosis or apoptosis. Science 343:1357-1360.
Ni HM, Chao X, Kaseff J, Deng F, Wang S, Shi YH, Li T, Ding WX, Jaeschke H (2019) Receptor-interacting serine/threonine-protein kinase 3 (RIPK3)-mixed lineage kinase domain-like protein (mlkl)-mediated necroptosis contributes to ischemia-reperfusion injury of steatotic livers. Am J Pathol doi: 10.1016/j.ajpath.2019.03.010.
Oerlemans MI, Liu J, Arslan F, den Ouden K, van Middelaar BJ, Doevendans PA, Sluijter JP (2012) Inhibition of RIP1-dependent necrosis prevents adverse cardiac remodeling after myocardial ischemia-reperfusion in vivo. Basic Res 107:270.
Ofengeim D, Ito Y, Najafov A, Zhang Y, Shan B, De Witt JP, Ye J, Zhang X, Chang A, Vakifahmetoglu-Norberg H, Geng J, Py B, Zhou W, Amin P, Berlink Lima J, Qi C, Yu Q, Trapp B, Yuan J (2015) Activation of necroptosis in multiple sclerosis. Cell Rep 10:1836-1849.
Pan P, Cai Z, Zhuang C, Chen X, Chai Y (2019) Methodology of drug screening and target identification for new necroptosis inhibitors. J Pharm Anal 9:71-76.
Panda PK, Naik PP, Meher BR, Das DN, Mukhopadhyay S, Praharaj PP, Maiti TK, Bhutia SK (2018) PUMA dependent mitophagy by Abrus agglutinin contributes to apoptosis through ceramide generation. Biochim Biophys Acta Mol Cell Res 1865:480-495.
Polster BM, Fiskum G (2004) Mitochondrial mechanisms of neural cell apoptosis. J Neurochem 90:1281-1289.
Puzzo D, Lee L, Palmeri A, Calabrese G, Arancio O (2014) Behavioral assays with mouse models of Alzheimer's disease: practical considerations and guidelines. Biochem Pharmacol 88:450-467.
Sai K, Parsons C, House JS, Kathariou S, Ninomiya-Tsuji J (2019) Necroptosis mediators RIPK3 and MLKL suppress intracellular replication independently of host cell killing. J Cell Biol doi:10.1083/jcb.201810014.
Shi S, Verstegen MMA, Mezzanotte L, de Jonge J, Löwik CWGM, van der Laan LJW (2019) Necroptotic cell death in liver transplantation and underlying diseases: mechanisms and clinical perspective. Liver Transpl doi: 10.1002/lt.25488.
Song G, Ma Z, Liu D, Zhou J, Meng H, Zhou B, Qian D, Song Z (2019) Bone marrow-derived mesenchymal stem cells ameliorate severe acute pancreatitis by inhibiting necroptosis in rats. Mol Cell Biochem doi:10.1007/s11010-019-03546-3.
Sowndhararajan K, Deepa P, Kim M, Park SJ, Kim S (2018) Neuroprotective and cognitive enhancement potentials of baicalin: a review. Brain Sci doi: 10.3390/brainsci8060104.
Tuunanen J, Lukasiuk K, Halonen T, Pitkänen A (1999) Status epilepticus-induced neuronal damage in the rat amygdaloid complex: distribution, time-course and mechanisms. Neuroscience 94:473-495.
Wang H, Ren XY, Ma CM, Huang C, Zhou HT (2016) Correlation between bone marrow stromal stem cells and apoptosis in epilepsy. Zhongguo Zuzhi Gongcheng Yanjiu 20:4117-4122.
Wang Z, Feng J, Yu J, Chen G (2019) FKBP12 mediates necroptosis by initiating RIPK1-RIPK3-MLKL signal transduction in response to TNF receptor 1 ligation. J Cell Sci doi:10.1242/jcs.227777.
Wu JR, Wang J, Zhou SK, Yang L, Yin JL, Cao JP, Cheng YB (2015) Necrostatin-1 protection of dopaminergic neurons. Neural Regen Res 10:1120-1124.
Xu F, Zhang G, Yin J, Zhang Q, Ge MY, Peng L, Wang S, Li Y (2019) Fluoxetine mitigating late-stage cognition and neurobehavior impairment induced by cerebral ischemia reperfusion injury through inhibiting ERS-mediated neurons apoptosis in the hippocampus. Behav Brain Res doi: 10.1016/j.bbr.2019.111952.
Xu X, Chua KW, Chua CC, Liu CF, Hamdy RC, Chua BH (2010) Synergistic protective effects of humanin and necrostatin-1 on hypoxia and ischemia/reperfusion injury. Brain Res 1355:189-194.
Yang C, Li T, Xue H, Wang L, Deng L, Xie Y, Bai X, Xin D, Yuan H, Qiu J, Wang Z, Li G (2018) Inhibition of necroptosis rescues sah-induced synaptic impairments in hippocampus via CREB-BDNF pathway. Front Neurosci 12:990.
Yang M, Kholmukhamedov A, Schulte ML, Cooley BC, Scoggins NO, Wood JP, Cameron SJ, Morrell CN, Jobe SM, Silverstein RL (2018) Platelet CD36 signaling through ERK5 promotes caspase-dependent procoagulant activity and fibrin deposition in vivo. Blood Adv 2:2848-2861.
Yang SH, Shin J, Shin NN, Hwang JH, Hong SC, Park K, Lee JW, Lee S, Baek S, Kim K, Cho Kim Y (2019) A small molecule Nec-1 directly induces amyloid clearance in the brains of aged APP/PS1 mice. Sci Rep 9:4183.
Yang Y, Jiang G, Zhang P, Fan J (2015) Programmed cell death and its role in inflammation. Mil Med Res 2:12.
You Z, Savitz SI, Yang J, Degterev A, Yuan J, Cuny GD, Moskowitz MA, Whalen MJ (2008) Necrostatin-1 reduces histopathology and improves functional outcome after controlled cortical impact in mice. Journal of cerebral blood flow and metabolism. J Cereb Blood Flow Metab 28:1564-1573.
Yuan S, Yu Z, Zhang Z, Zhang J, Zhang P, Li X, Li H, Shen H, Chen G (2019) RIP3 participates in early brain injury after experimental subarachnoid hemorrhage in rats by inducing necroptosis. Neurobiol Dis doi: 10.1016/j.nbd.2019.05.004.
Zeng L, Da X, Gu H, Yang D, Yang S, Xiang L (2007) High antinoisephotoacoustic tomography based on a modified filtered backprojection algorithm with combination wavelet. Med Phys 34:556-563.
Zeng Y, Da X, Wang Y, Yin B, Chen Q (2004) Photoacoustic and ultrasonic coimage with a linear transducer array. Opt Lett 29:1760-1762.
Zhang HF, Maslov K, Stoica G, Wang LV (2006) Functional photoacoustic microscopy for high-resolution and noninvasive in vivo imaging. Nat Biotechnol 24:848-851.
Zhang T, Balachandran S (2019) Bayonets over bombs: RIPK3 and MLKL restrict without triggering necroptosis. J Cell Biol doi:10.1083/jcb.201905047.
Zhang X, Dowling JP, Zhang J (2019a) RIPK1 can mediate apoptosis in addition to necroptosis during embryonic development. Cell Death Dis 10:245.
Zhang YF, Xiong TQ, Tan BH, Song Y, Li SL, Yang LB, Li YC (2014) Pilocarpine-induced epilepsy is associated with actin cytoskeleton reorganization in the mossy fiber-CA3 synapses. Epilepsy Res 108:379-389.
Zhang YY, Liu WN, Li YQ, Zhang XJ, Yang J, Luo XJ, Peng J (2019b) Ligustroflavone reduces necroptosis in rat brain after ischemic stroke through targeting RIPK1/RIPK3/MLKL pathway. Naunyn Schmiedebergs Arch Pharmacol doi: 10.1007/s00210-019-01656-9.
Zhou X, Chu X, Yuan H, Qiu J, Zhao C, Xin D, Li T, Ma W, Wang H, Wang Z, Wang D (2019) Mesenchymal stem cell derived EVs mediate neuroprotection after spinal cord injury in rats via the microRNA-21-5p/FasL gene axis. Biomed Pharmacother 115:108818.

P-Reviewers: Faiq M, Lovejoy DB; C-Editor: Zhao M; S-Editors: Wang J, Li CH; L-Editors: Patel B, de Souza M, Qiu Y, Song LP; T-Editor: Jia Y